Fluctuation-Response Theorem for the Active Noisy Oscillator of the Hair-Cell Bundle

L. Dinis,[1,2] P. Martin,[1] J. Barral,[1] J. Prost,[1,3] and J. F. Joanny[1]

[1]*Laboratoire Physico-Chimie Curie, CNRS, Institut Curie, UPMC, 26 rue d'Ulm, F-75248 Paris Cedex 05, France*
[2]*Grupo Interdisciplinar de Sistemas Complejos (GISC) and Universidad Complutense de Madrid, Madrid 28040, Spain*
[3]*E.S.P.C.I., 10 rue Vauquelin, 75231 Paris Cedex 05, France*

(Received 7 May 2012; published 18 October 2012)

The hair bundle of sensory cells in the vertebrate ear provides an example of a noisy oscillator close to a Hopf bifurcation. The analysis of the data from both spontaneous and forced oscillations shows a strong violation of the fluctuation-dissipation theorem, revealing the presence of an underlying active process that keeps the system out of equilibrium. Nevertheless, we show that a generalized fluctuation-dissipation theorem, valid for nonequilibrium steady states, is fulfilled within the limits of our experimental accuracy and computational approximations, when the adequate conjugate degrees of freedom are chosen.

DOI: 10.1103/PhysRevLett.109.160602 PACS numbers: 05.70.Ln, 05.40.−a, 05.45.−a, 87.16.dj

The fluctuation-dissipation theorem (FDT) is the cornerstone of linear response theory for systems at thermal equilibrium [1]: it relates the response to small perturbations to the correlations of spontaneous fluctuations and connects the microscopic dynamics of the system to the macroscopic transport coefficients, such as diffusion constant, conductivity, absorption rates, etc.

Many systems operate far from thermodynamic equilibrium and therefore, do not obey the FDT. One illustrative example is given by the hair-cell bundle. The hair bundle operates as a mechanical antenna that protrudes from the apical surface of each hair cell in the inner ear of vertebrates [2,3]. Hearing starts when sound evoked deflections of this organelle are transduced into electrical signals that then travel to the brain. Composed of cylindrical protrusions—the stereocilia—that are arranged in rows of increasing heights, the hair bundle displays a staircase pattern. Stereocilia are interlinked near their tips by fine oblique filaments. Tip-link tension controls the open probability of mechanosensitive ion channels. The hair cell can power noisy spontaneous oscillations of its hair bundle that display a spectacular violation of the FDT [4]. The behavior of the hair bundle has been described by the generic normal form of a dynamical system that operates on the stable side of a Hopf bifurcation [5]. In this Letter, we focus on this particular class of out-of-equilibrium systems.

Several generalizations of the FDT to nonequilibrium systems have been proposed [6–9]. The generalized fluctuation-dissipation theorem (GFDT) of Prost *et al.* [10] applies to systems with Markovian dynamics in a nonequilibrium steady state. Applying the GFDT to experimental measurements on the hair bundle, we show here that a proper choice of variables restores a relation between spontaneous fluctuations and linear response.

Details of the experiment are found in Refs. [4,11,12]. The oscillatory movement of a hair bundle was monitored with a glass fiber attached to its tip (Fig. 1(a)). The fiber was used both to exert sinusoidal forces and to report hair-bundle noisy oscillations. The power spectrum $\tilde{C}_{xx}(\omega) = \int C_{xx}(t)e^{i\omega t}dt$ of spontaneous hair-bundle position x, which is the Fourier transform of the correlation function $C_{xx}(t) = \langle x(t)x(0)\rangle$, displays a broad peak centered at a characteristic frequency $\nu_0 = \omega_0/2\pi \simeq 6$ Hz (Fig. 1(b)). For stimulation by external sinusoidal forces $f(t)$, the linear response function $\tilde{\chi} = \tilde{\chi}' + i\tilde{\chi}''$ is defined at each angular frequency ω by $\langle\tilde{x}(\omega)\rangle = \tilde{\chi}(\omega)\tilde{f}(\omega)$, where tildes denote Fourier components. Its imaginary part $\tilde{\chi}''(\omega)$ is proportional to the work received by the system from the external force for stimulation at a frequency ω [13]. At thermal equilibrium, with our definition of the Fourier transform, $\tilde{\chi}''(\omega)$ must always be positive (for $\omega \geq 0$).

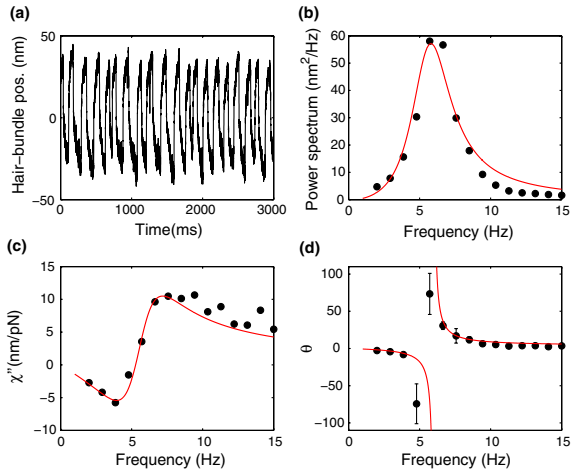

FIG. 1 (color online). Experimental data from a hair bundle: (a) Spontaneous hair-bundle oscillation. (b) Power spectral density $\tilde{C}_{xx}(\nu)$ averaged from 15 different trajectories as a function of frequency ν. (c) Imaginary part of the response function $\tilde{\chi}''_{xx}(\nu)$. Thin red lines (b–c) correspond to a simultaneous fit of $\tilde{C}_{xx}(\nu)$ and $\tilde{\chi}''_{xx}(\nu)$ to theoretical expressions derived from Eq. (4). (d) Fluctuation-response ratio θ as defined in Eq. (2) fitted to theoretical expression given in Ref. [4].

Remarkably, in the case of the oscillatory bundle, $\tilde{\chi}''(\omega)$ changes sign near ν_0, as shown in Fig. 1(c). At low frequencies, the work received by the bundle is negative, meaning that energy is transferred from the hair bundle to the fiber. An energy consuming or active process must, thus, be at work to power hair-bundle movements.

At thermal equilibrium, the FDT relates the imaginary part of the response function to the power spectrum of spontaneous fluctuations for a degree of freedom x

$$\tilde{C}_{xx}(\omega) = 2kT\frac{\tilde{\chi}''_{xx}(\omega)}{\omega}, \tag{1}$$

where T is the temperature and k the Boltzmann constant. Departure from equilibrium can be characterized by the fluctuation-response ratio

$$\theta = \frac{\omega\tilde{C}_{xx}(\omega)}{2kT\tilde{\chi}''_{xx}(\omega)}, \tag{2}$$

sometimes called the effective temperature (in units of the room temperature T). This ratio equals one when the system is at equilibrium. In an out-of-equilibrium system, θ might depend on frequency and be either positive or negative. For the hair bundle, the fluctuation-response ratio θ shown in Fig. 1(d) depends on frequency and presents a striking divergence in the vicinity of $\nu_0 = \omega_0/2\pi$, corresponding to the sign change of $\tilde{\chi}''_{xx}(\nu)$. However, if the GFDT applies, a fluctuation-response relation is restored with an appropriate choice of the conjugate variable X to the external force [14]

$$\tilde{\chi}_{XX}(\omega) - \tilde{\chi}_{XX}(-\omega) = i\omega\tilde{C}_{XX}(\omega). \tag{3}$$

The behavior of the hair bundle for small deflections has been described as a two variable dynamical system:

$$\frac{d}{dt}\begin{pmatrix} x \\ y \end{pmatrix} = \begin{pmatrix} -r & \omega_0 \\ -\omega_0 & -r \end{pmatrix}\begin{pmatrix} x \\ y \end{pmatrix} + \begin{pmatrix} f_x \\ 0 \end{pmatrix} + \begin{pmatrix} \eta_x \\ \eta_y \end{pmatrix}. \tag{4}$$

The variable x is the deflection of the hair bundle, $r = k/\lambda$ is a damping rate, where λ and k are, respectively, the effective drag coefficient and the stiffness of the bundle, $f_x = f_{\text{ext}}/\lambda$, where f_{ext} is the external force on the hair bundle. The second degree of freedom y is related to the force exerted by the active process within the hair bundle and couples to the displacement x. The noises η_x and η_y describe fluctuations in the system. We treat the two Langevin forces as white noises so that the dynamical system is Markovian. At the low frequencies of the experiment (~ 10 Hz), we expect noise correlation times to be sufficiently short that the noises can be considered as delta-correlated. Non-Markovian effects are expected at higher frequencies only, as discussed below. Equation (4) is to be understood as a renormalized expression, valid for providing two point correlation functions and linear responses, of a more complex nonlinear problem [5,12,15]. As a result, the noises η_x and η_y are, in general, correlated. However, experimentally, the cross correlation turned out to be very small and the two noises are effectively independent. The noise correlations are written as $\langle\eta_x(t)\eta_x(t')\rangle = \sigma_{\eta_x}\delta(t-t')$, $\langle\eta_y(t)\eta_y(t')\rangle = \sigma_{\eta_y}\delta(t-t')$.

The dynamical system described by Eq. (4) is the canonical form of a system close to a Hopf bifurcation [16]. If $r > 0$, it displays damped spontaneous oscillations of frequency ω_0. The expressions for the power spectrum and the complex response function to an external force f_x can be readily computed from this model and were used for a global fit of the experimental data with a unique set of parameters r, ω_0, σ_{η_x}, and σ_{η_y} in Fig. 1 (the real part of the response function is not shown).

With the choice of x as conjugate variable of the external force f_x, the FDT is violated (Fig. 1(c)). This is a strong signature of a nonequilibrium behavior. Nevertheless, the dynamics of Eq. (4) being Markovian, the GFDT of Prost *et al.* [10] holds for the correct conjugate variable X of the external force. In the case of the two-dimensional linear system at hand, Eq. 5 in Ref. [10] yields:

$$\begin{pmatrix} X \\ Y \end{pmatrix} = [A^{-1}]^{\mathrm{T}}\Sigma_A^{-1}\begin{pmatrix} x \\ y \end{pmatrix} \tag{5}$$

with

$$A = -\begin{pmatrix} -r & \omega_0 \\ -\omega_0 & -r \end{pmatrix}, \qquad \Sigma_A = \begin{pmatrix} \langle x^2\rangle_{\text{ss}} & \langle xy\rangle_{\text{ss}} \\ \langle xy\rangle_{\text{ss}} & \langle y^2\rangle_{\text{ss}} \end{pmatrix}, \tag{6}$$

where the averages in the matrix Σ_A are calculated in the steady state. A direct test of the GFDT would thus, require a measurement of the internal degree of freedom y, which is not experimentally accessible.

To circumvent this limitation, we propose three different approaches. On the one hand, using the measured x value, we estimate the hidden variable either by computing the linear combination $z = y\omega_0 - rx$ of x and y using a denoising procedure, or by an optimization technique. On the other hand, we directly evaluate the correlations involving z which are sufficient to test the validity of the GFDT. Using the variable z, we write the dynamical system as

$$\begin{aligned}\frac{d}{dt}\begin{pmatrix} x \\ z \end{pmatrix} &= \begin{pmatrix} 0 & 1 \\ -(r^2+\omega_0^2) & -2r \end{pmatrix}\begin{pmatrix} x \\ z \end{pmatrix} + \begin{pmatrix} f_x + \eta_x \\ f_z + \eta_z \end{pmatrix} \\ &\equiv -R\begin{pmatrix} x \\ z \end{pmatrix} + \begin{pmatrix} f_x + \eta_x \\ f_z + \eta_z \end{pmatrix},\end{aligned} \tag{7}$$

where the noise and force in the z equation are $\eta_z = -r\eta_x + \omega_0\eta_y$ and $f_z = -rf_x$.

In the absence of external force, $\frac{dx}{dt} = z + \eta_x$. We can, therefore, estimate the value of z by filtering the time series of the speed data, eliminating the high-frequency noise: at each point of the trajectory, the value of the speed is calculated by averaging over the N preceding points, where N is such that the averaging effectively filters signals faster than 60 Hz. This frequency is several times higher than the

spontaneous oscillation frequency of the bundle $\nu_0 \simeq 6$ Hz and could be varied without much effect on the final results as long as it is high enough (≥ 30 Hz) to preserve the waveform of hair-bundle oscillation and low enough (≤ 90 Hz) to get rid of most of the high-frequency noise. Denoising implicitly relies on the assumption that the velocity $\dot{x}$ can be split into a variable z with exponentially decaying correlations plus white noise. As can be checked at very low frequencies, it only gives an approximation z_e of the actual variable z.

Once the variables x and z_e are obtained, we apply the GFDT to the system described by Eq. (7), which is also Markovian. The correlation matrix for the x and z variables in Fourier space is then approximated by

$$\tilde{C}_{\vec{x}\,\vec{x}}(\omega) \simeq \begin{pmatrix} \langle \tilde{x}(\omega)\tilde{x}^*(\omega)\rangle & \langle \tilde{x}(\omega)\tilde{z}_e^*(\omega)\rangle \\ \langle \tilde{z}_e\omega)\tilde{x}^*(\omega)\rangle & \langle \tilde{z}_e(\omega)\tilde{z}_e^*(\omega)\rangle \end{pmatrix}, \tag{8}$$

where the star denotes a complex conjugate.

We compute $\tilde{x}(\omega)$ and $\tilde{z}_e(\omega)$ using the FFT algorithm on the experimental data. The matrix R is obtained from the values of r and ω_0 and then used to perform the change of variables

$$\vec{X} \equiv \begin{pmatrix} X \\ Z_e \end{pmatrix} = [R^{-1}]^{\mathrm{T}}\Sigma^{-1}\begin{pmatrix} x \\ z_e \end{pmatrix} \tag{9}$$

where

$$\Sigma = \begin{pmatrix} \langle x^2\rangle_{\mathrm{ss}} & \langle xz_e\rangle_{\mathrm{ss}} \\ \langle z_e x\rangle_{\mathrm{ss}} & \langle z_e^2\rangle_{\mathrm{ss}} \end{pmatrix}.$$

In the new variables, the power spectrum reads

$$\tilde{C}_{\vec{X}\,\vec{X}}(\omega) = [R^{-1}]^{\mathrm{T}}\Sigma^{-1}\tilde{C}_{\vec{x}\,\vec{x}}(\omega)[\Sigma^{-1}]^{\mathrm{T}}R^{-1} \tag{10}$$

and the response function

$$\tilde{\chi}_{\vec{X}\,\vec{X}}(\omega) = [R^{-1}]^{\mathrm{T}}\Sigma^{-1}\tilde{\chi}_{\vec{x}\,\vec{x}}(\omega) = [R^{-1}]^{\mathrm{T}}\Sigma^{-1}[R - i\omega]^{-1}. \tag{11}$$

The GFDT [10] then imposes a relation between fluctuations and the response given by Eq. (3). In particular, for the first diagonal element, we expect the fluctuation-response ratio:

$$\theta = \frac{\omega\tilde{C}_{XX}(\omega)}{2\tilde{\chi}''_{XX}(\omega)} = 1. \tag{12}$$

In Fig. 2 (black circles), we plot the fluctuation-response ratio θ evaluated from the experimental data. We find that θ wiggles about the value 1, within a range that stretches from 0.5 to 2. This is a remarkable behavior considering that, when fluctuations and response were evaluated with the hair-bundle position x as the relevant degree of freedom, the fluctuation-response ratio changed sign and diverged near the characteristic frequency of spontaneous oscillations (Fig. 1(d)). Although the GFDT imposes that θ be precisely equal to 1, numerical simulations shown below demonstrate that the experimental data are compatible with the GFDT.

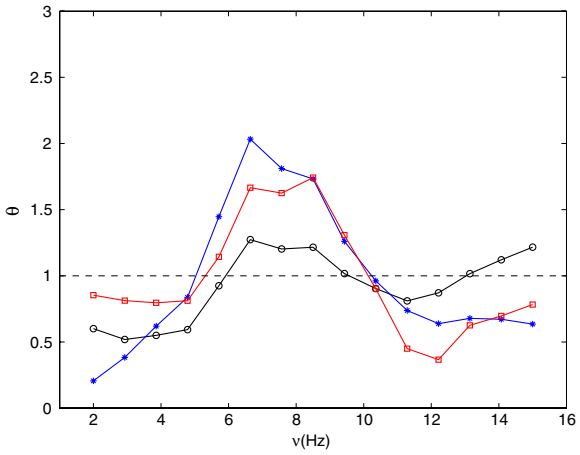

FIG. 2 (color online). The fluctuation-response ratio θ vs. stimulation frequency ν using the three different methods explained in the text. Black open circle: denoising of z, red open square: estimation of $\tilde{C}_{\vec{x}\,\vec{z}}(\omega)$, blue asterisk: y estimation by maximization of probability. Note that the power spectra were smoothed out to eliminate some of the noise by a moving average algorithm. Lines are just guides for the eye.

We then used an inference method to estimate the variable y from the measured trajectories. The assumption of Gaussian white noises for η_x and η_y in Eq. (4) implies that the combinations $\dot{x} + rx - \omega_0 y$ and $\dot{y} + \omega_0 y + rx$ are Gaussian variables for spontaneous oscillations ($f_x = 0$). Discretizing the evolution [Eq. (4)] in N time steps Δt, we find

$$\begin{aligned} x_{n+1} - x_n + \Delta t(rx_n - \omega_0 y_n) &\sim \mathcal{N}(0, \sigma_{\eta_x}\Delta t), \\ y_{n+1} - y_n + \Delta t(rx_n - \omega_0 y_n) &\sim \mathcal{N}(0, \sigma_{\eta_x}\Delta t), \end{aligned} \tag{13}$$

where $\mathcal{N}(\mu, \sigma^2)$ denotes the normal distribution of average μ and variance σ^2. The probability $\rho(\{x_n, y_n\})$ of observing a discrete full trajectory $\{x_n, y_n\}_{n=1}^{n=N}$ is then a product of $2N$ Gaussian distributions. Maximizing this probability with respect to the y_n variables ($\partial\rho/\partial y_n = 0$, $\forall\ n$) gives a linear system of equations for the most likely trajectory $\{y_n\}$ in terms of the measured variable $\{x_n\}$ and the parameters r, ω_0, σ_{η_x} and σ_{η_y}. We use this estimated trajectory to perform the change of variables [Eq. (5)] required for the GFDT. The resulting θ is depicted in Fig. 2.

Our third approach to test the GFDT avoids any y estimation by directly calculating the correlation matrix from the measured data. Only the first element of the matrix $\tilde{C}_{xx}(\omega)$ can be directly obtained from the experimental data. To estimate the elements involving z, we proceed as follows. Fourier transforming Eq. (7) for $f_x = 0$, we get $\tilde{z}(\omega) = -i\omega\tilde{x}(\omega) - \tilde{\eta}_x(\omega)$, which we use to calculate the cross correlation

$$\tilde{C}_{xz}(\omega) = i\omega\tilde{C}_{xx}(\omega) - \langle\tilde{x}(\omega)\tilde{\eta}_x(-\omega)\rangle. \tag{14}$$

The second term in Eq. (14) is evaluated by means of the evolution equation [Eq. (7)] giving

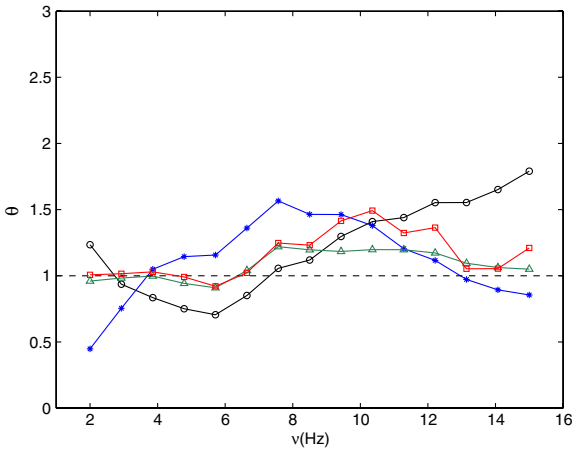

FIG. 3 (color online). θ ratio computed after the change of variables prescribed by the GFDT, from simulated data. Computed using black open circle: $\tilde{x}$ and $\tilde{z}_e$, blue asterisk: $\tilde{x}$ and $\tilde{y}$ estimated by probability maximization, red open square: direct $\tilde{C}_{\tilde{x}\tilde{y}}(\omega)$ estimation and green upward triangle: $\tilde{x}$ and actual (no filtering nor estimation) $\tilde{y}$. Simulations where done with $r = 10.2\ \mathrm{s}^{-1}$, $\omega_0 = 36.5\ \mathrm{rad/s}$ and $\sigma_x = 10\,000\ \mathrm{nm}^2/\mathrm{s}$ and $\sigma_y = 10\,000\ \mathrm{nm}^2/\mathrm{s}$. Lines are just guides for the eye.

$$\tilde{C}_{xz}(\omega) = i\omega\tilde{C}_{xx}(\omega) - \sigma_{\eta_x}\frac{r - i\omega}{r^2 + \omega_0^2 - \omega^2 - 2ri\omega}, \quad (15)$$

where the only unknown parameter is the noise intensity σ_{η_x}. However, from Eq. (7), one can show that $\sigma_{\eta_x} = -2\Sigma_{12}$. Following the same lines, both $\tilde{C}_{zx}(\omega)$ and $\tilde{C}_{zz}(\omega)$ are expressed in terms of $\tilde{C}_{xx}(\omega)$, r, ω_0, and Σ_{12}. Finally, we estimate Σ from the data by noting that $\Sigma_{11} = \langle x(0)^2\rangle = C_{xx}(t=0)$, $\Sigma_{12} = \langle x(0)z(0)\rangle = \frac{dC_{xx}(t)}{dt}|_{t=0}$ or alternatively by fitting the power spectrum expressed as a function of Σ_{11} and Σ_{12}, noting that $\Sigma_{22} = (r^2 + \omega_0^2)\Sigma_{11}$.

Once Σ, R, and $\tilde{C}_{\tilde{x}\dot{\tilde{x}}}(\omega)$ are known, we insert them into Eq. (10) and compute the fluctuation-response ratio θ as in Eq. (12) (Fig. 2).

In order to asses the impact of the three different estimation methods, we performed numerical simulations with parameters similar to those of the experiment and repeated the procedure using both our estimates and the actual y value, which is available in simulations. The simulations were performed using the Euler–Mayurama method [17] to solve Eq. (4). As expected, results in Fig. 3 show that the agreement with the theorem is best when the actual variable y is used. However, even then, we still observe deviations of θ by about 25% due to a lack of averaging. In addition, both the moving-average procedure and the inference method imply a dependence on past history, and thus, introduce some degree of non-Markovianity that might explain further departure from the GFDT. Because experiments and simulations show similar deviations of the fluctuation-response ratio from 1, we consider that it is as close to 1 as possible, in view of the inherent limitations associated with the methods that we used to estimate this ratio.

In conclusion, we showed that the GFDT [10] applies to oscillatory hair-cell bundles. Although the hair bundle provides a compelling example of a complex biological system that operates away from thermal equilibrium, its linear mechanical response is related to steady-state fluctuations with the appropriate choice of a conjugate variable to the external force. This relation holds for frequencies close to the frequency of spontaneous oscillation, at which the hair bundle can be described by a two-dimensional dynamical system operating near a Hopf bifurcation. This property affords a means to estimate the hidden variable that underlies the activity of the hair bundle. Because the hair bundle must satisfy the hypotheses of the GFDT, our results support the description of the hair bundle as a single noisy oscillator governed by Markovian dynamics and therefore, go against a viscoelasticity of the hair bundle in the range of frequencies that we studied. At higher frequencies, however, the hair bundle could become non-Markovian, due mainly to memory resulting from viscoelasticity [18] or from colored fluctuations in the opening and closing of the transduction channels [15]. Channel clatter is only expected at frequencies above $\sim$1 kHz [15], where a departure from the GFDT could be observed.

Our work relates to the experiments of Ref. [19] which test the same GFDT for an experimental system consisting of a Brownian particle in a toroidal optical trap. In contrast to our study where we have to assume a Hopf bifurcation dynamics with noise, in the optical trap experiment the evolution equation is known, as the potential felt by the particle is also applied using the trap.

We have provided three methods for the estimation of correlations involving the nonmeasured degree of freedom. Both the denoising and the inference methods can be directly applied to other noisy systems. It would be, however, desirable to perform experiments where, in addition to the displacement, the dynamics of the active term can be controlled and measured. A good candidate for an additional measurement is the ionic current that flows through the bundle, which is known to influence either the myosin motors that generate the force inside the bundle or the transduction channel to which the motors are attached [20].

We would like to thank F. Jülicher for discussions. L. D. acknowledges support from grants MOSAICO and ENFASIS (FIS2011-22644) and the POSDEXT-MEC program (Spanish Government) and Universidad de Sevilla.

[1] H. Callen and T. Welton, Phys. Rev. **83**, 34 (1951).
[2] A. J. Hudspeth, Nature (London) **341**, 397 (1989)
[3] J. Barral and P. Martin, Curr. Opin. Otolaryngol. Head Neck Surg. **19**, 369 (2011).

[4] P. Martin, A. J. Hudspeth, and F. Julicher, Proc. Natl. Acad. Sci. U.S.A. **98**, 14 380 (2001).
[5] F. Julicher, K. Dierkes, B. Lindner, J. Prost, and P. Martin, Eur. Phys. J. E **29**, 449 (2009).
[6] G. S. Agarwal, Z. Phys. **252**, 25 (1972).
[7] R. Chetrite, G. Falkovich, and K. Gawedzki, J. Stat. Mech. (2008) P08 005.
[8] T. Speck and U. Seifert, Europhys. Lett. **74**, 391 (2006).
[9] M. Baiesi, C. Maes, and B. Wynants, Phys. Rev. Lett. **103**, 010 602 (2009).
[10] J. Prost, J.-F. Joanny, and J. M. R. Parrondo, Phys. Rev. Lett. **103**, 090 601 (2009).
[11] P. Martin and A. J. Hudspeth, Proc. Natl. Acad. Sci. U.S.A. **96**, 14 306 (1999).
[12] J.-Y. Tinevez, F. Jülicher, and P. Martin, Biophys. J. **93**, 4053 (2007).
[13] D. Chandler, *Introduction to Modern Statistical Mechanics* (Oxford University, New York, 1987).
[14] Note that we used here a different sign convention than in Ref. [10], both for the definition of the Fourier transform and the definition of the variable X.
[15] B. Nadrowski, P. Martin, and F. Julicher, Proc. Natl. Acad. Sci. U.S.A. **101**, 12 195 (2004).
[16] D. Strogatz, *Non-Linear Dynamics and Chaos* (Addison-Wesley, Reading, MA, 1997).
[17] R. Mannella, in *Stochastic Processes in Physics Chemistry and Biology*, edited by T. P. Jan, A. Freund (Springer, Berlin, 2000), p. 353.
[18] A. S. Kozlov, D. Andor-Ardó, and A. J. Hudspeth, Proc. Natl. Acad. Sci. U.S.A. **109**, 2896 (2012).
[19] J. R. Gomez-Solano, A. Petrosyan, and S. Ciliberto, J. Phys. Conf. Ser. **297**, 012 006 (2011).
[20] T. Duke, J. Phys. Condens. Matter **15**, S1747 (2003).